

ARTICLES

**Balance of the Deactivation Channels of the First Excited Singlet State of Phenols: Effect of Alkyl Substitution, Sterical Hindrance, and Solvent Polarity**

R. Hermann,\* G. R. Mahalaxmi, T. Jochum, S. Naumov,† and O. Brede

*University of Leipzig, Interdisciplinary Group Time-Resolved Spectroscopy, Permoserstrasse 15, D-04303 Leipzig, Germany*

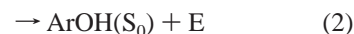
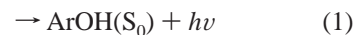
*Received: October 26, 2001; In Final Form: December 16, 2001*

On the basis of laser flash photolysis with detection by picosecond and nanosecond emission as well as absorption spectroscopy, a quantitative description is given of all the deactivation channels of the first excited singlet state of phenols ArOH(S<sub>1</sub>) such as fluorescence, intersystem crossing to the triplet system (ISC), chemical dissociation into radicals, and radiationless internal conversion (IC). For this purpose, various phenols with different alkyl substitution patterns (mono to 3-fold substitution with methyl and /or *tert*-butyl groups) were studied in solvents of increasing polarity: cyclohexane, *n*-butyl chloride, tetrahydrofuran, ethanol, methanol, acetonitrile, and water. The fluorescence lifetimes of the phenols were found to range from a few tens of picoseconds up to a few nanoseconds, correlating with fluorescence quantum yields between 10<sup>-1</sup> and 10<sup>-3</sup>, at room temperature. With a probability less than 0.1, the photodissociation of ArOH(S<sub>1</sub>) was found to be nearly unaffected by changing the type of solvent. As a result of the ISC the triplet yields amount to 0.2–0.3, with smaller values in nonpolar and the larger ones in polar media. As a very marked exception, sterically hindered phenols (2,6-di-*tert*-butyl substituted) behave quite differently: they exhibit extremely short living fluorescences, show no ISC, and, radiationless, are only deactivated by internal conversion. This complete physical energy dissipation makes the sterically hindered phenols ideal light quenchers.

**Introduction**

Because of their antioxidant properties, the photophysics and photochemistry of phenols are of great interest for various fields of science and technology. To establish what happens after a phenol (ArOH) molecule has been excited by an UV photon, with regard to the relaxation of the first excited singlet state

ArOH(S<sub>1</sub>) the competing reactions 1–5 should be considered.

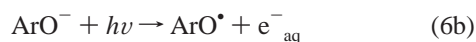
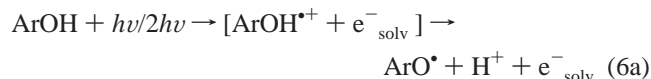


Whereas emission measurements allow easy, direct access to

\* To whom correspondence should be addressed. E-mail: hermann@mpgag.uni-leipzig.de.

† Institute of Surface Modification, Permoserstrasse 15, D-4303 Leipzig, Germany.

the fluorescence channel (reaction 1), the characterization of intersystem crossing (ISC) to the triplet system (reaction 3), and of photodissociation (reaction 4) by optical absorption spectroscopy is difficult because of the indifferent properties of the phenol triplets and the problem of exactly determining phenoxyl radical formation due to singlet dissociation (reaction 4). Furthermore, the possible photoionization (reaction 6), which appears at higher laser power or at high pH-values in aqueous solution, complicates the situation.



Our experimental conditions were chosen as such that photoionization (reaction 6) and self-quenching (reaction 5) do not play a significant role. There is no easy and direct access to the yield of the radiationless internal conversion (IC, reaction 2), which represents the vibrational relaxation (VR) and energy ( $E$ ) dissipation in the solvent.

Since the pioneering flash photolysis work of Land et al.,<sup>1</sup> who directly detected phenoxyl radicals, reports have been published on the generation and kinetics of phenoxyl radicals, excited singlet, and triplet states of methoxy-substituted phenols in solution,<sup>2</sup> isotope effects on the photophysical properties of phenol in 3-methylpentane,<sup>3</sup> excited triplet state chemistry in water,<sup>4</sup> temperature effects on fluorescence lifetimes,<sup>3,5,6</sup> and solvent effects on singlet state deactivation.<sup>7</sup> For nonpolar solutions, Grabner et al.<sup>8</sup> systematically investigated the deactivation pathways of the first excited singlet state of phenol and methylated derivatives of phenol with different substitution patterns and reported quantum yields of the radiationless deactivation (reaction 2) of more than 0.5. It was found that methyl substituents affect the photophysical behavior only marginally.

Because substituents, such as methyl- and *tert*-butyl-groups, only slightly change the electronic structure of phenolic molecules, the corresponding electronic transitions observed of the phenols studied can be assumed to be of the same type. On the other hand, electronic effects caused by electron-donating or electron-withdrawing substituents, steric effects, and the solvent nature certainly ought to influence the balance of the  $S_1$  relaxation pathways. As already stated by Köhler et al.,<sup>7</sup> in extreme cases, e.g., for protic solvents, interaction between surrounding molecules and the phenoxyl group may lead to the formation of ground-state complexes which modify the picture of phenol excitation and the relaxation of the  $S_1$  state. Such effects and more generally also the competition between all relaxation channels of ArOH ( $S_1$ ) are definitely reflected by the fluorescence kinetics observed. Hence, most of the reports on the photochemistry of phenol singlet excited state are based on fluorescence measurements.

Because of the complexity of the problem and the variety of factors of influence, a general treatment must be separately performed for each of the singlet relaxation processes. Therefore, we directly investigated all the other  $S_1$  deactivation pathways except for internal conversion (reaction 2) for the various phenols and solvents using time-resolved emission and absorption spectroscopy. The remaining radiationless internal conversion ArOH( $S_1$ ) was then determined by a difference calculation using these experimental data. Finally, fluorescence lifetime measurements in binary solvent mixtures and photolysis experi-

ments for two phenols with para substituents of opposite electronic effects are reported.

## Experimental Section

To determine quantum yields, spectral and kinetic data of the phenol triplet state, and the yield of the phenoxyl radical formed via the excited (singlet) states, real-time nanosecond-laser photolysis was applied. The solutions were photolyzed by the fourth harmonics (266 nm) of a Quanta-Ray GCR-11 Nd:YAG laser (Spectra Physics). Pulses of <3 ns duration (FWHM) with energies of 0.5 mJ were used. The involvement of two-photon processes was ruled out by running the laser at such low power that no signal contribution generated via ionic species (phenol radical cations, solvated electrons) could be observed. This was proofed by checking the signal influence against oxygen (phenol radical cations are not quenched by oxygen). Solutions flowed continuously through a 5 mm quartz sample cell. All samples were saturated with  $N_2$  except for the ionization of phenolates, where  $N_2O$  was used as electron scavenger. All measurements were performed at room temperature. The optical detection system consisted of a pulsed Xenon lamp (XBO 450, Osram), a monochromator (SpectraPro 275, Acton Research), an R955 photomultiplier tube (Hamamatsu Photonics) or a fast Si-photodiode with 1 GHz amplification, and a 500 MHz digitizing oscilloscope (DSA 602 A, Tektronix). The laser power was monitored for every pulse using a bypath with a fast Si-photodiode.

Fluorescence lifetimes were measured with an amplified (CPA) 10 Hz Ti:Sapphire femtosecond-UV laser system. After excitation with a 250 fs (FWHM) UV laser pulse at 253 nm, a highly sensitive streak camera C5680/M5676 (Hamamatsu Photonics) recorded the fluorescence kinetics. A time resolution of 1 ps was achieved for the emission studies by applying the deconvolution technique.<sup>9</sup> Fluorescence quantum yields were calculated from radiative lifetime data derived from stationary emission (spectrofluorimeter FluoroMax-2, Instruments S. A., Jobin Yvon-Spex) and ground state absorption (UV/VIS-spectrophotometer UV-2101 PC, Shimadzu) spectra.

Absorption measurements were performed by a pump-probe setup using the 253 nm photons of the fs-Ti:Sapphire laser system for excitation. The white light continuum was generated by focusing a small fraction of the basic radiation of the laser system (760 nm) in a  $10 \times 10 \text{ mm}^2$  water (50%  $D_2O$ ) cell. Spectra were recorded using a CCD detector (Princeton Instruments TE/CCD-1100-PB/UV AR). A 1.5 m rail table served as a delay line for spectra recording at different times. The overall time resolution for absorption studies was about 0.5 ps.

The following *tert*-butyl-substituted phenols were investigated: 2-, 3-, and 4-*tert*-butylphenol (2-, 3-, 4-TBP); 2,4-, 3,5-, and 2,6-di-*tert*-butylphenol (2,4-, 3,5-, 2,6-DTBP), as well as 2,4,6-tri-*tert*-butylphenol (2,4,6-TTBP). Additionally, phenol, 2,4,6-trimethylphenol (2,4,6-TMeP), 4-methoxyphenol (4-MeOP), and 4-cyanophenol (4-CNP), as well as phenols with more than one substituent (such as methyl-, methoxy- and *tert*-butyl-groups) in different positions, were studied. All phenols were of highest analytical grade (Aldrich) and partially further purified by distillation (2-TBP), sublimation (di-*tert*-butylphenols) or preparative chromatography.  $\beta$ -Carotene (Aldrich, 95%) was used as received. Water, methanol (MeOH), ethanol (EtOH), tetrahydrofuran (THF), acetonitrile (MeCN), *n*-butyl chloride (BuCl), and cyclohexane (c-Hex) of highest spectroscopic grade were chosen as solvents. Cyclohexane and *n*-butyl chloride were further purified by passing them through A4 and

$\times 13$  molecular sieves followed by distillation. Water was purified by a Millipore filtration system (Milli Q Plus).

**Quantum Chemistry.** Mulliken charges and dipole moments were calculated and frequency analysis conducted for all molecules using DFT B3LYP/6-31 G(d) level for ground state and RCIS for excited state geometric parameters.<sup>10,11</sup>

## Results and Discussion

**Kinetics of Fluorescence.** Fluorescence decay kinetics monitors all the relaxation processes competing for the excited singlet state of a molecule. For example, light-induced emission measurements can provide provisional, crude information about excited singlet state deactivations, i.e., the overall lifetime of this state. As concluded from literature data,<sup>8</sup> phenol itself and its methyl-substituted derivatives seem to exhibit similar kinetic behavior, as reproduced in our recent measurements. Because sterically hindered phenols are often used as antioxidants, we introduced bulky substituents one by one into the phenol molecule and undertook time-resolved fluorescence studies with mono-, di-, and tri-*tert*-butyl-substituted phenols with different substitution patterns, excited into their lowest singlet state  $\text{ArOH}(S_1)$ , such as monosubstituted compounds 2-, 3-, and 4-*tert*-butylphenol (2-, 3-, 4-TBP), di-substituted molecules 2,4-, 3,5-, and 2,6-di-*tert*-butylphenol (2,4-, 3,5-, 2,6-DTBP), as well as 2,4,6-tri-*tert*-butylphenol (2,4,6-TTBP) in solvents of different polarity. For comparison and adjustment to known data, phenol, 2,4,6-trimethylphenol (2,4,6-TMeP), and a few other combined-substituted phenols, as well as (in order to consider electronic effects) 4-methoxyphenol (4-MeOP) and 4-cyanophenol (4-CNP), were studied in cyclohexane, ethanol, and acetonitrile. According to the changing fluorescence quantum yields, the experiments were performed with solutions of  $10^{-5}$ – $10^{-4}$  mol  $\text{dm}^{-3}$  of the phenols in solvents of different polarity. The experimentally observed fluorescence lifetimes obtained by a single-exponential regression at room temperature are listed in Tables 1 and 2. From these room temperature data the following conclusions can be drawn:

(i) For a fixed phenol type, in aprotic solvents the fluorescence lifetime  $\tau_f$  nearly always increases with rising solvent polarity (characterized by the dielectric constant or also by the empirical Reichardt parameter  $E_T^N$  (ref 12)).

(ii) Compared to the nonsubstituted phenol, substitution by methyl- or *tert*-butyl groups in the meta- or para-position only slightly affects the fluorescence lifetimes.

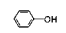
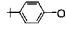
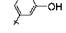
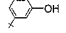
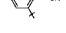
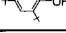
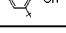
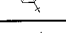
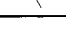


(iii) In the case of the so-called sterically hindered phenols—*tert*-butyl-substituted in both ortho positions (2,6-DTBP and 2,4,6-TTBP)—there is a drastic lifetime reduction to values in the picosecond time domain ( $\tau_f$  between 30 and 250 ps). No systematics, i.e., no real solvent influence, was found for this systems.

(iv) In accordance with the data reported by Grabner et al.,<sup>8</sup> the fluorescence kinetics of methylated phenols in nonpolar media were found to be close to each other and (especially for the high-substituted 2,4,6-trimethylphenol, 2,4,6-TMeP) the fluorescence lifetime was similar to that of phenol itself (cf. Table 2).

(v) For phenols, steric effects determine the fluorescence lifetimes such that  $\tau_f$  decreases with increasing hindrance of the phenolic group. Therefore in Table 1 the *tert*-butyl-substituted phenols are ordered by increasing steric hindrance.

(vi) The compound 4-cyanophenol (4-CNP) with an electron-withdrawing group shows a relatively long lifetime and much more intense fluorescence. In 4-methoxyphenol (4-MeOP) with

**TABLE 1: Fluorescence Lifetimes (in Nanoseconds) of Phenols ( $c = 5 \times 10^{-4}$  mol  $\text{dm}^{-3}$ ) in Different Media at Room Temperature<sup>a</sup>**

Compound	Structure $E_T^N =$	c-Hex $\epsilon = 2.0$ 0.006	BuCl $\epsilon = 7.0$	THF $\epsilon = 7.6$ 0.207	EtOH $\epsilon = 24$ 0.654	MeOH $\epsilon = 33$ 0.762	MeCN $\epsilon = 38$ 0.460	Water $\epsilon = 78$ 1.00
Phenol		2.2	3.9	4.5	4.6	5.2	5.5	3.1
4-TBP		1.4	3.4	3.9	5.3	4.7	5.1	2.9
3-TBP		1.8	3.4	4.7	5.2	4.9	5.5	3.1
3,5-DTBP		1.0	2.2	3.0	2.8	2.7	3.4	1.3
2-TBP		0.460	1.8	3.3	4.8	4.0	5.0	2.2
2,4-DTBP		0.405	1.0	3.5	4.3	3.8	4.3	1.7
2,6-DTBP		0.050	0.060	0.046	0.035	0.030	0.051	insolub
2,4,6-TTBP		0.123	0.119	0.090	0.085	0.071	0.090	insolub
2,4,6-TMeP		1.8			2.2		2.1	
4-MeOP		1.3			2.2		2.8	
4-CNP		5.2			2.8		5.7	

<sup>a</sup> As polarity parameters, dielectric constants  $\epsilon$  for 20 °C and Reichardt's empirical  $E_T^N$  values<sup>12</sup> are included. The error in the lifetime estimation is about  $\pm 10\%$ . <sup>b</sup>  $E_T^N$  denotes an empirical parameter of solvent polarity (Reichardt scale).<sup>12</sup> Values are given for the solvents used.

an electron-donating group,  $\tau_f$  is only marginally affected by the nature of the solvent.

(vii) From the fluorescence lifetime data given in Table 2, it can be seen that *tert*-butyl substitution in one or two ortho-positions causes a drastic lifetime decrease where any para- and meta-substituents have no marked effect compared to the basic phenol itself.

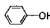
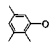
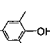
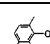
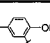
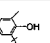
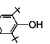
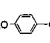
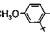
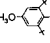
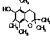
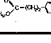
A few measurements were carried out in *n*-heptadecane (viscosity = 3.34 cp at 20 °C; the viscosity of the other nonpolar solvents used is typically around 0.5 cp) to study the solvent viscosity effect. Here only minor lifetime deviations were obtained ( $\tau_f = 2.5$  ns for phenol,  $\tau_f = 513$  ps for 2-TBP, and  $\tau_f = 65$  ps for 2,6-DTBP). Decreasing the temperature from 20 to 10 °C caused the fluorescence lifetime of 2-TBP to increase from 513 ps up to 615 ps.

To compare substitution at different positions and to identify trends, the fluorescence kinetics of some other selected phenols were measured in nonpolar media at room temperature and are summarized in Table 2, together with literature data. These values confirm our above conclusions. However, at first sight no real systematics could be derived for the influence of the substituents.

As also shown by our measurements, the fluorescence behavior of aromatics also depends on the chemical and physical properties of the surroundings. Because of the very complex factors of influence (protic and aprotic media, polarity, viscosity, and dipole moment phenomena), theoretical interpretation is difficult. For simplicity's sake, in the following we will distinguish between general continuum and specific solvent effects.

For general solvent–solute excited-state interactions, an approach is given by the Lippert–Mataga equation,<sup>13</sup> which

**TABLE 2: Fluorescence Lifetime at Room Temperature of Substituted Phenols in Nonpolar Solvents<sup>a</sup>**

Compound	Structure	$\tau_f$ solvent /ref/	$\tau_f$ c-Hex	$\tau_f$ BuCl
Phenol		2.3 ns <sup>n-hex-ane</sup> /8/ 1.9 ns <sup>3-me-pent</sup> /3/	2.2 ns	3.9 ns
2,3,5-TMeP		660 ps <sup>n-hexane</sup> /8/	640 ps	
2,4,6-TMeP		2.1 ns <sup>n-hexane</sup> /8/	1.8 ns	
2,3,6-TMeP			1.7 ns	
4-Me-2-TBP			660 ps	
6-Me-2-TBP			1.80 ns	
4-Me-2,6-DTBP			240 ps	260 ps
4-MeOP		1.8 ns <sup>MeOH/MeCN</sup> /2/	1.3 ns	285 ps
2-TB-4-MeOP			900 ps	
2,6TB-4MeOP			1.3 ns	1.2 ns
TROLOX			1.3 ns	
IRGANOX-1076 <sup>(R)</sup>			240 ps	

<sup>a</sup> IRGANOX-1076: *n*-octadecyl-3-(3,5-di-*tert*-butyl-4-hydroxyphenyl)-propionate.

describes the collective influence of the entire set of surrounding molecules on the solute singlet states. In this equation

$$hc\Delta\tilde{\nu} = 2 \Delta f(\mu^* - \mu)^2/a^3 \quad (7)$$

$\Delta\tilde{\nu}$  denotes the frequency shift (in  $\text{cm}^{-1}$ ) between absorption and emission,  $\Delta f$  is the orientation polarization,  $a$  is the radius of the cavity in which the fluorophore resides, and  $\mu^*$  and  $\mu$  are the excited and ground state dipole moments, respectively. Such general effects are determined by the polarizability of the solvent molecules (according to the refractive index  $n$ ) and the molecular solvent polarizability (resulting from the reorientation of the solvent dipoles). The latter property is expressed by the static dielectric constant  $\epsilon$  and the perturbation is thus related to the high and low-frequency dielectric constants of the medium, viewed as a continuum. These physical constants reflect the freedom of motion of the electrons in the solvent molecules, as well as the dipole moment ( $\mu$ ) of these molecules. Such electrostatic interactions are of a long-range nature. The refractive indices of the solvents used in this study are all around  $n = (1.3 \pm 0.1)$  and, therefore, effects due to differences in the  $n$ -values in a first approximation could be neglected for the interpretation of our data.

In contrast to the nonspecific continuum interaction, *specific interactions* are molded by the excited state and molecular properties of the neighboring molecules, and determined by the specific chemical properties of both the solute singlet states and the surrounding solvent molecules.<sup>14</sup> Such specific effects, which are usually manifested in short-range interactions, can be caused by hydrogen bonding, acid–base chemistry, proton and charge-transfer interactions, and solvent-dependent aggregation (charge-transfer complexes and electron-pair donor acceptor complexes),

to name but a few. Specific effects often have larger interaction energies and are characterized by defined stoichiometric and structural relationships. Hence, they depend on the defined chemical structure of the solvent molecules and the solute singlet states and, therefore, yield directional forces which can be saturated. It should be noted, that the influence resulting from specific solvent–solute interactions frequently exceeds that due to general interactions.

Therefore, in the following the solvent influence on the  $\text{ArOH}(S_1)$  decay will be initially considered from the following angles: (i) the interaction of hydrogen bonds of solvent and solute molecules, (ii) the effect of polarity (dielectric constant), and (iii) the efficiency of energy dissipation to the solvent via vibrational relaxations (VR).

Under protic conditions hydrogen bonds are formed with the phenol solute molecules, i.e., the specific solvent effect dominates. Looking at nonprotic media, polarity effects, such as general continuum solvent–solute interaction phenomena, predominate. In water and alcohol solutions, hydrogen bonds are formed with the hydroxyl group of the phenols. Here, phenol acts as proton donor and consequently electronic charge is transferred from the solvent molecule to the phenolic oxygen, which stabilizes the phenol-excited state. This effect dominates the negative charge (electron) flux from the phenolic oxygen to the aromatic ring as well as the influence of the increase in the dipole momentum caused by excitation. Therefore, the fluorescence lifetime prolongation indicates the higher stability of the  $S_1$  state in the presence of hydrogen bonds compared to the nonpolar or aprotic situation. Indeed, the fluorescence lifetimes measured in water and in alcohols are longer than in the aprotic solvents (see Table 1). Otherwise, fluorescence lifetimes measured in aqueous solution are shorter than in alcohols. This indicates more efficient nonradiative relaxation in water, which is probably caused by the more intense overtones of the OH-vibrations in water compared to alcohols (as expressed by the corresponding OH-vibrational bands at around  $3400 \text{ cm}^{-1}$  obtained by IR spectroscopy<sup>15</sup>). Such strong OH-vibrations considerably increase the yield of the nonradiative IC-deactivation route (see discussion below). In acetonitrile, tetrahydrofuran, *n*-butyl chloride, and cyclohexane, the polarity effect is responsible for the gradual influence on the fluorescence lifetime within these solvents.

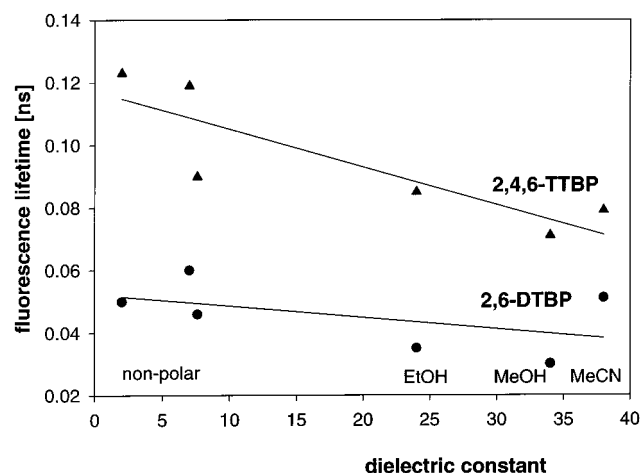
Therefore, the stability of phenol-excited states in polar solvents is even higher than for less-polar surroundings, i.e., the fluorescence lifetime increases with increasing dielectric constant (Table 1). However, this does not hold for the situation in the sterically hindered phenols. Here, no marked polarity influence on  $T_f$  was observed. For this type of phenol, effects by sterical hindrance seem to take precedence over solvent effects. For 2,6-DTBP and 2,4,6-TTBP, Figure 1 shows this effect using a plot of  $\tau_f$  vs  $\epsilon$  of the solvents used.

Given the effect of dipole moment interaction between solvent and solute molecules, we performed quantum chemical estimations. Excitation into the singlet spin system causes the induction of a usually larger dipole moment than in the ground state. The larger the dipole moment of the excited state, the longer fluorescence lifetimes observed. Owing to long-range dipole–dipole interaction, polar solvents increase the dipole moment of the excited state of the solute molecules. Dipole moments  $\mu$  and Mulliken charges  $Q(\text{O})$  at the phenolic oxygen atom for the singlet ground and excited states of the studied compounds as calculated via RCIS are presented in Table 3. Although the dipole moment is enlarged by excitation into the excited singlet state, the changes are small and do not exhibit a clear correlation



**TABLE 3: B3LYP/6-31G(d) Calculated Rotation and Valence OH Frequencies ( $\nu$ ) with Corresponding Oscillator Strength ( $f$ : Proportional to the Intensity of Selected Transition) and Configuration Interaction Single RCIS/6-31G(d) Calculated Changes of Mulliken Charge ( $\Delta Q$ ) and Dipole Moment ( $\Delta\mu$ ) in First Excited Singlet State**

compound	$\tau_f$ (c-Hex) $\epsilon = 2.0$	$\nu$ [ $\text{cm}^{-1}$ ] valence	$f$ intensity	$\nu$ [ $\text{cm}^{-1}$ ] rot	$f$ intensity	$\frac{Q(O)}{Q(O)^*}$	$\Delta Q$	$\frac{\mu}{\mu^*}$	$\Delta\mu$ [debye]
phenol	2.2 ns	3751	38	359	123	-0.762	0.026	1.496	0.003
4-TBP	1.4 ns	3751	42	357	107	-0.736	0.026	1.499	0.026
3-TBP	1.8 ns	3,75	36	359	122	-0.765	0.032	1.562	-0.169
3,5-DTBP	1.0 ns	3754	34	361	95	-0.766	0.030	1.801	0.024
2-TBP	460 ps	3748	197	175	40	-0.734	0.030	2.090	0.024
2,4-DTBP	405 ps	3859	202	157	28	-0.794	0.028	1.969	-0.007
2,6-DTBP	50 ps	3857	218	92	21	-0.766	0.027	1.962	0.301
2,4,6-TTBP	123 ps	3856	225	93	23	-0.801	0.031	2.071	0.048
2,4,6-TMeP	1.8 ns	3780	38	265	67	-0.774	0.030	2.377	0.055
4-MeOP	1.3 ns	3757	41	310	121	-0.803	0.028	2.044	0.089
						-0.772		2.092	
						-0.783		1.548	
						-0.753		1.603	
						-0.768		0.564	
						-0.740		0.653	

**Figure 1.** Relation between fluorescence lifetimes and dielectric constant of the solvent for the two sterically hindered phenols 2,4-DTBP and 2,4,6-TTBP. Solvents: cyclohexane, chlorobutane, tetrahydrofuran, ethanol, methanol, and acetonitrile.

with the fluorescence lifetimes measured. The negative charge flow from the hydroxyl group into the aromatic ring via excitation is in the same range for all the phenols studied. Therefore we conclude that influence by dipole interaction does not cause the fluorescence lifetime modification observed.

To find out more about the nature of the hydrogen bond effect on the relaxation of the phenol first excited states, we recorded the fluorescence lifetimes of 4-TBP in different mixtures of cyclohexane and ethanol. This ought to help distinguish between local interactions in nonpolar media and long-range interactions. Molecules with OH-groups may act as both good proton donors and good proton acceptors, and thus form hydrogen bonds easily. The fluorescence lifetimes are drastically increased by adding only small amounts of ethanol to cyclohexane solutions. About 0.15 mol % ethanol enlarged the fluorescence lifetimes of nonhindered phenols to the double. They remain constant as of an ethanol content of about 5 mol %. Such an ethanol content is too low to affect the refractive index and the dielectric constant of the solvent. Therefore, we conclude that the electrostatic interaction between the phenol-excited singlet states and the ethanol molecules is of minor importance and the lifetime influence observed has to be attributed to hydrogen bond interactions. The above-mentioned saturation effect even at low

ethanol content confirms the well-known fact that hydrogen bond formation is very efficient, even taking place when there are only a few surrounding protic molecules. The accepting modes for internal conversion are mainly the OH-vibrations, the highest energy modes in the system. Hydrogen bonding decreases their energy considerably and so the rate of the IC decreases too. OH-vibrational modes play a dominant role in the relaxation of phenol-excited states.

To mention but a few, the sterically hindered phenols exhibit fluorescence lifetimes down to 50 ps in cyclohexane and 35 ps in ethanol in the case of 2,6-DTBP as well as 123 ps in cyclohexane and 85 ps in ethanol in the case of 2,4,6-TTBP, respectively (see Table 1). For this type of phenol, solvent interaction does not cause the lifetime to decrease, whereas the steric hindrance of the OH-group seems to be important. Other 2,6-di-*tert*-butyl-substituted phenols were not studied in detail but ought to show similar behavior (Table 2). Quantum chemical vibrational analysis (cf. Table 3) revealed considerably higher intensities (values of around 200) for the valence OH frequencies around  $3800\text{ cm}^{-1}$  for the sterically hindered phenols compared to the less or nonhindered ones (intensities between 35 and 50). The spectral position of this band is only slightly varied for the compounds analyzed. Therefore, it can be concluded that steric hindrance strongly increased the OH-vibrations, hence sharply increasing the probability of any of the nonradiative decay routes. When considering a few other bulky substituted phenols in nonpolar solvents (Table 2), such as 4-Me-2,6-DTBP ( $\tau_f = 240\text{ ps}$ ) and 2,6-DTB-4MeOP ( $\tau_f = 1.3\text{ ns}$ ), it can be seen that another heterogroup, such as a methyl- or a methoxy-group (via electronic effects), increases the fluorescence lifetime considerably. In the case of the long-tail para-substituted technical stabilizer IRGANOX-1076 ( $\tau_f = 240\text{ ps}$ ), the steric hindrance remains dominant.

**Measurements of Phenol Singlet Absorptions by Picosecond Absorption Spectroscopy.** Applying the pump and probe technique, the singlet state kinetics of phenols were studied by picosecond absorption measurements using 253 nm excitation. The phenols exhibit a characteristic short-lived broad absorption in the visible spectral range, usually between 400 and 650 nm, caused by  $S_1-S_N$  excitation. Figure 2a,b shows typical  $S_1-S_N$  absorption time profiles for 4-Me-2,6-DTBP in cyclohexane as well as those for BuCl solutions. Figure 2c shows the singlet absorption time profile for a solution of phenol in cyclohexane

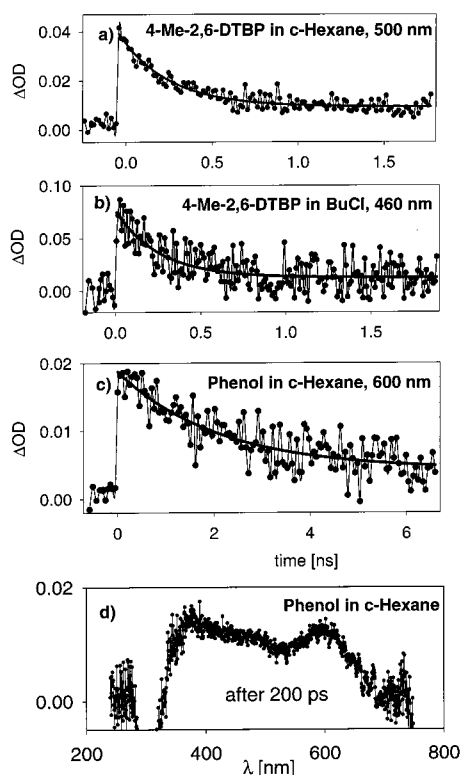


**Figure 2.**  $S_1$ – $S_N$  absorption time profiles obtained by picosecond pump–probe studies for 4-Me-2,6-DTBP in cyclohexane (Figure 2a) and butyl chloride (Figure 2b) and phenol in cyclohexane (Figure 2c) solutions. Figure 2d shows the absorption spectrum of phenol in cyclohexane measured 200 ps after the excitation pulse.

**TABLE 4: Comparison of the Excited Singlet State Lifetime of Several Phenols in Cyclohexane and Chlorobutane Obtained by Direct Fluorescence Detection ( $\tau_f$ ) and via the Corresponding Singlet Absorption ( $\tau_{abs}$ )**

compound	spectral range $S_1$ – $S_N$ absorption	cyclohexane		<i>n</i> -butyl chloride	
		$\tau_f$	$\tau_{abs}$	$\tau_f$	$\tau_{abs}$
phenol	425–600 nm	2.2 ns	2.2 ns	3.9 ns	1.4 ns
4-TBP	420–560 nm	1.4 ns	250 ps	3.4 ns	1.1 ns
3,5-DTBP	460–600 nm	1.0 ns	1.1 ns	1.3 ns	1.1 ns
4-MeO-P	460–630 nm	1.3 ns	1.2 ns	290 ps	1.7 ns
3,5-DTBP-4MeOP	460–510 nm	1.3 ns	1.4 ns	1.2 ns	800 ps
4-Me-2,6-DTBP	470–550 nm	240 ps	280 ps	260 ps	280 ps
4-CNP	no absorption				

and Figure 2d a representative absorption spectrum taken 200 ps after the laser pulse. Table 4 gives singlet lifetimes obtained by fluorescence measurements as well as by pump and probe  $S_1$ – $S_N$  absorption detection. It can be seen that both methods yielded similar data.

**Fluorescence Quantum Yields.** Quantum yields of fluorescence were determined via the radiative lifetime calculated from the stationary absorption and emission spectra of the phenols. According to Strickler and Berg<sup>16</sup> the radiative lifetime  $k_{rad}$  is given by

$$k_{rad} = 1/\tau_0 = 2.88 \times 10^{-9} (n^2) [(\langle \tilde{\nu}_f \rangle^{-3})]^{-1} g_f/g_u \int \epsilon_T d \ln \tilde{\nu} \quad (8)$$

where  $\tilde{\nu}$  is the wavenumber in  $[\text{cm}^{-1}]$ ,  $n$  the refractive index of the solvent, and  $\tau_0$  the radiative lifetime. Then the fluorescence quantum yield results from  $\Phi_f = \tau_f/\tau_0$ .

In eq 8 the term  $[(\langle \tilde{\nu}_f \rangle^{-3})]^{-1}$  represents the integral over the fluorescence spectrum and  $\int \epsilon_T d \ln \tilde{\nu}$  is the integral over the absorption spectrum. For singlet–singlet transitions, a ratio  $g_f/g_u = 1$  is assumed. For further details see ref 16.

**TABLE 5: Radiative Rate Constants  $k_{rad}$  and “Strickler–Berg Values” Obtained for Phenols in Cyclohexane, Acetonitrile, and Ethanol**

compound	solvent	$\int \epsilon_T(\tilde{\nu})/\tilde{\nu} d \ln \tilde{\nu}$ [ $\text{mol}^{-1} \text{cm}^4$ ]	$1/\langle \nu_f^{-3} \rangle$ [ $\times 10^{13} \text{cm}^{-3}$ ]	Strickler–Berg $k_{rad} = 1/\tau_0$ [ $\times 10^7 \text{s}^{-1}$ ]
phenol	c-Hex	171.46	3.72	3.76
	EtOH	216.95	3.58	4.14
	MeCN	156.36	3.61	2.92
4-TBP	c-Hex	195.38	3.53	4.06
	EtOH	229.46	3.32	4.06
	MeCN	185.64	3.44	3.30
2,6-DTBP	c-Hex	169.71	3.06	3.06
	EtOH	146.60	2.93	2.29
	MeCN	191.35	3.07	3.04
3,5-DTBP	c-Hex	203.47	3.52	4.21
	EtOH	227.68	3.42	4.15
	MeCN	160.56	3.53	2.93
2,4,6-TTBP	c-Hex	234.47	2.92	4.03
	EtOH	209.57	3.01	3.49
	MeCN	235.08	2.90	3.53
2,4,6-TMeP	c-Hex	252.48	3.33	4.95
	EtOH	221.84	3.22	3.81
	MeCN	228.64	3.31	3.91
4-MeOP	c-Hex	283.01	2.89	4.82
	EtOH	385.55	2.72	5.59
	MeCN	356.04	2.75	5.06
4-CNP	c-Hex	1790.14	3.34	35.2
	EtOH	1774.62	3.13	29.6
	MeCN	1481.90	3.34	25.6

**TABLE 6: Quantum Yields of Triplet Formation (ISC) Determined by Sensitization Experiments in the Solvents Cyclohexane, Acetonitrile, and Ethanol<sup>a</sup>**

compound	triplet quantum yield $\Phi_T$		
	cyclohexane	acetonitrile	ethanol
phenol	0.27	0.5	0.67
4-TBP	0.27	0.47	0.7
3,5-DTBP	0.23	0.27	0.33
2,6-DTBP	0	0	0
2,4,6-TTBP	0	0	0
2,4,6-TMeP	0.5	0.45	0.5
4-MeOP	0.6	0.55	0.67
4-CNP	0.17	0.56	0.57

<sup>a</sup> Values are within  $\pm 10\%$  accuracy.

All values calculated from the experimental steady-state spectra are listed in Table 5. Applying eq 8, the radiative rate constant  $k_{rad} = 1/\tau_0$  of the phenols in cyclohexane, acetonitrile, and ethanol were calculated and listed in the column “Strickler–Berg”. The fluorescence quantum yields finally calculated are summarized in Table 8 for the three solvents cyclohexane, acetonitrile, and ethanol. Our value for the fluorescence quantum yield of phenol in cyclohexane ( $\Phi_f = 0.083$ ) is in good agreement with reported data for phenol in *n*-hexane or 3-methylpentane ( $\Phi_f = 0.075$ ).<sup>8</sup> For a few selected compounds, we also determined fluorescence quantum yields in dioxane solution:  $\Phi_f(\text{phenol}) = 0.084$ ,  $\Phi_f(4\text{-TBP}) = 0.11$ ,  $\Phi_f(3,5\text{-DTBP}) = 0.079$ , and  $\Phi_f(2,4,6\text{-TTBP}) = 0.007$ .

As reported above, the interpretation of the given fluorescence effects caused by the solvent nature and the molecular structure of the solute on the  $\text{ArOH}(S_1)$  deactivation is more or less qualitative. A thorough analysis of the deactivation mechanism entails a detailed study of all nonradiative processes (equations 2–5). According to whether the transition is spin-allowed or spin-forbidden, the radiationless transitions are known as internal conversion (IC) (transition between states of the same multiplicity) or intersystem crossing (ISC) (transition between states of

**TABLE 7: Extinction Coefficients  $\epsilon_T$  and Maxima of the Absorption of the Phenoxyl Radical for Solvents of Different Nature<sup>a</sup>**

compound	water		cyclohexane		ethanol
	$\lambda_{\max}$ [nm]	$\epsilon_{T400\text{nm}}$ [mol <sup>-1</sup> cm <sup>-1</sup> ]	$\lambda_{\max}$ [nm]	$\epsilon_{T400\text{nm}}$ [mol <sup>-1</sup> cm <sup>-1</sup> ]	$\epsilon_{T400\text{nm}}$ [mol <sup>-1</sup> cm <sup>-1</sup> ]
phenol	400	2625	400	3830	2350
4-TBP	409	3080	405	3830	2740
3-TBP	412	1560	409	1510	1650
3,5-DTBP	430	2040	420	2570	1560
2-TBP	397	1830	398	1770	1780
2,4-DTBP	406	3160	404	4340	1760
2,6-DTBP	396	1150	396	1890	670
2,4,6-TTBP	400	2830	400	3430	2930

<sup>a</sup> The phenols are denoted as D = di, T = *tert*, TT = tri-*tert*, and BP = butyl phenol.

**TABLE 8: Quantum Yields of Deactivation Channels in Cyclohexane, Ethanol, and Acetonitrile<sup>a</sup>**

c-hexane	$\Phi_T \pm 10\%$	$\Phi_f \pm 10\%$	$\Phi_D \pm 20\%$	$1 - (\Phi_T + \Phi_f + \Phi_D)$	$\tau_f$	$k_{IC} [\times 10^9 \text{ s}^{-1}]$
phenol	0.27	0.083	0.07	0.58	2.2 ns	0.26
4-TBP	0.27	0.057	0.04	0.63	1.4 ns	0.45
3,5-DTBP	0.23	0.042	0.05	0.68	1.0 ns	0.68
2,6-DTBP	0	0.002	0.01	0.99	50 ps	19.8
2,4,6-TTBP	0	0.005	0.01	0.98	123 ps	7.97
2,4,6-TMeP	0.5	0.099	0.05	0.35	1.8 ns	0.18
4-MeOP	0.6	0.1	0.05	0.25	2.3 ns	0.11
4-CNP	0.17	0.825	0.05	negligible	5.2 ns	
ethanol	$\Phi_T \pm 10\%$	$\Phi_f \pm 10\%$	$\Phi_D \pm 20\%$	$1 - (\Phi_T + \Phi_f + \Phi_D)$	$\tau_f$	$k_{IC} [\times 10^9 \text{ s}^{-1}]$
phenol	0.67	0.19	0.07	0.07	4.6 ns	0.015
4-TBP	0.7	0.215	0.04	0.045	5.3 ns	0.0085
3,5-DTBP	0.33	0.12	0.05	0.5	2.8 ns	0.18
2,6-DTBP	0	0	0.01	0.99	35 ps	28.3
2,4,6-TTBP	0	0	0.01	0.99	85 ps	11.6
2,4,6-TMeP	0.5	0.084	0.05	0.37	2.2 ns	0.17
4-MeOP	0.67	0.13	0.05	0.16	2.2 ns	0.073
4-CNP	0.57	0.38	0.05	negligible	2.8 ns	
acetonitrile	$\Phi_T \pm 10\%$	$\Phi_f \pm 10\%$	$\Phi_D \pm 20\%$	$1 - (\Phi_T + \Phi_f + \Phi_D)$	$\tau_f$	$k_{IC} [\times 10^9 \text{ s}^{-1}]$
phenol	0.5	0.16	0.07	0.27	5.5 ns	0.049
4-TBP	0.47	0.16	0.04	0.34	5.1 ns	0.067
3,5-DTBP	0.27	0.08	0.05	0.6	3.4 ns	0.176
2,6-DTBP	0	0	0.01	0.99	51 ps	19.4
2,4,6-TTBP	0	0	0.01	0.99	90 ps	11
2,4,6-TMeP	0.45	0.082	0.05	0.41	2.1 ns	0.195
4-MeOP	0.55	0.1	0.05	0.3	2.8 ns	0.11
4-CNP	0.56	0.39	0.05	negligible	5.7 ns	

<sup>a</sup>  $k_{IC}$  values were calculated via  $k_{IC} = \Phi_{IC}/\tau_f$ .

different multiplicity), both in connection with vibrational relaxation (VR). In liquids, vibrational relaxation from an excited state, e.g., the  $S_1$ , to the vibrational ground state  $S_0$ , is very rapid ( $k_{VR} \times 10^{13} \text{ s}^{-1}$  for liquids<sup>17</sup>) and the excess energy is converted into heat through collisions with solvent molecules. Because ISC (reaction 3) often competes efficiently with IC (reaction 2), the rapid and radiationless vibration relaxation of the triplet state may also occur.

**Triplet Quantum Yields of the Phenols in Cyclohexane, Acetonitrile, and Ethanol Solutions.** The triplet-triplet absorption spectrum of phenol in water was measured by Bent and Hayon<sup>4</sup> using a frequency-quadrupled Nd:YAG laser. The phenol T-T absorption spectra typically exhibit one UV-band around 240 nm and a very weak but much broader one in the visible spectral range around 400 nm<sup>2,4,8</sup>, where the triplet extinction coefficient for phenol is  $\epsilon_{400\text{nm}} < 1,000 \text{ M}^{-1} \text{ cm}^{-1}$ .<sup>8</sup> Using higher laser power ( $> 1 \text{ mJ}$ ), the  $T_1-T_n$ -spectrum appears superimposed by the absorption of the phenoxyl radical ( $\lambda_{\max} \sim 400, \sim 290, \text{ and } \sim 245 \text{ nm}$ ) and the solvated electron as products of the two-photon reaction channel (cf. reaction 6). For a laser energy of only 0.5 mJ per pulse, insufficient for photoionization, the transient spectra obtained were sensitive to oxygen as expected for triplet states, in contrast to phenoxyl

radicals. The triplet lifetimes were found to be in the range of a few microseconds. Typical time profiles taken at 240 nm under oxygen and oxygen-free conditions are shown in Figure 3 for a solution of 1 mM phenol in acetonitrile. For the two sterically hindered phenols (2,6-DTBP and 2,4,6-TTBP) and for 4-CNP, no direct triplet formation was observed by excitation with 266 nm photons. Because of the phenol self-absorption and superpositions with other absorptions, the UV band is still inappropriate for a quantitative treatment. Moreover, in the visible range the low triplet extinction coefficients and the unspecific triplet spectra severely complicate the quantitative determination of the quantum yields.

Therefore, to circumvent these difficulties, we performed a sensitization experiment using the triplet energy transfer from ArOH to  $\beta$ -carotene ( $\beta$ -C): rather low triplet energy and pronounced  $T_1-T_n$  absorption spectrum in the visible range.<sup>18</sup> Since this triplet spectrum is superimposed with the red-shifted self-absorption of  $\beta$ -carotene, we adjusted the  $\beta$ -C triplet extinction coefficient by a further sensitization experiment with benzophenone (reaction 9), a substance which exhibits complete ISC.<sup>19</sup> Monitoring the experiment at  $\lambda = 530 \text{ nm}$ , the BP( $T_1$ ) immediately formed can be seen, which decays under the formation of the  $\beta$ -C( $T_1$ ): cf. curve 2 of Figure 4. A direct

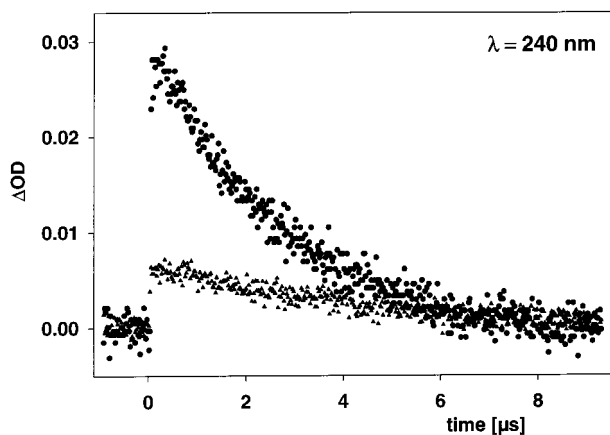


**Figure 3.** Signal of the ArOH( $T_1$ ) state at  $\lambda = 240$  nm taken in the 266 nm photolysis of a solution of  $10^{-3}$  mol  $\text{dm}^{-3}$  phenol in acetonitrile, laser energy 1 mJ/pulse. The upper triplet signal is obtained in  $\text{N}_2$ -purged solution, the lower one shows the remaining transient kinetic after triplet quenching in oxygen-saturated solution.

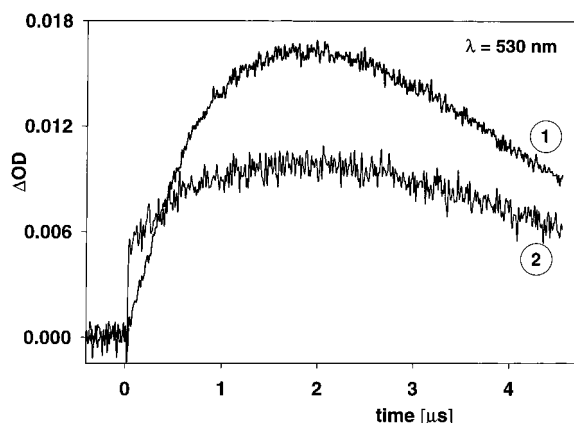
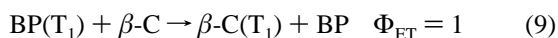
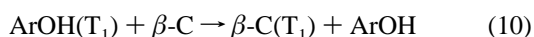


**Figure 4.** Time profile of the  $\beta$ -carotene first excited triplet state at  $\lambda = 530$  nm measured in the laser photolysis of a solution of  $2 \times 10^{-3}$  mol  $\text{dm}^{-3}$  phenol and  $2 \times 10^{-4}$  mol  $\text{dm}^{-3}$   $\beta$ -carotene in acetonitrile (curve 1),  $\text{N}_2$ -purged solution, laser energy 0.5 mJ/pulse. Curve 2 shows the sensitization with benzophenone ( $10^{-4}$  mol  $\text{dm}^{-3}$ ) under conditions where the optical density of the sample is actually 10 times that of the phenol experiment.

comparison of the absorptions directly after the flash and after 1  $\mu\text{s}$  yields the required extinction coefficient. Figure 4 shows the time profiles of the  $\beta$ -carotene triplet  $T_1$ -state measured at 530 nm. Curve 1 displays the  $\beta$ -carotene triplet state formation via sensitization from benzophenone (reaction 9) and curve 2 shows the  $\beta$ -carotene triplet kinetic via sensitization from phenol (reaction 10) at 0.5 mJ excitation energy.



To determine the quantum yields of the phenol triplets, we performed the sensitization experiments according to eq 10.



The experiments were performed under optically matched conditions (reaction 11).

$$\text{OD}_{266 \text{ nm}}(\text{BP}) = \text{OD}_{266 \text{ nm}}(\text{ArOH}) \quad (11)$$

The comparably low self-absorption of  $\beta\text{-C}$  at 266 nm does not distort the experiment because its direct excitation does not result in triplet-excited molecules (fast isomerization of olefin bonds<sup>20</sup>).

Therefore, in solutions of  $2 \times 10^{-3}$  mol  $\text{dm}^{-3}$  phenol and  $2 \times 10^{-4}$  mol  $\text{dm}^{-3}$   $\beta$ -carotene, the 266 nm laser photolysis excites mainly ArOH molecules. Subsequently we observed the time-resolved formation of  $\beta\text{-C}(T_1)$  according to reaction 10 (cf. curve 1 of Figure 4).

The phenol triplet quantum yields  $\Phi_T(\text{ArOH})$  required were obtained by the ratio of the  $\Delta\text{OD}_{530 \text{ nm}}$ -values of  $\beta$ -carotene triplet formed via the energy transfer reactions 9 and 10 under the conditions mentioned above (equation 11):

$$\Phi_T(\text{ArOH}) = \frac{\Delta\text{OD}_{530 \text{ nm}}(\text{ArOH} \rightarrow \beta\text{-C}_{\text{reaction 10}})}{\Delta\text{OD}_{530 \text{ nm}}(\text{BP} \rightarrow \beta\text{-C}_{\text{reaction 9}})} \quad (12)$$

Phenol triplet quantum yields  $\Phi_T$  were thus determined for solutions in cyclohexane, acetonitrile and ethanol (cf. Table 6). In the case of phenol in cyclohexane ( $\Phi_T = 0.32$ ), *n*-hexane ( $\Phi_T = 0.24$ ) and ethanol ( $\Phi_T = 0.65$ ) and for 2,4,6-TMeP in *n*-hexane ( $\Phi_T = 0.21$ ), we were able to reproduce literature data.<sup>8,21</sup>

Analyzing the data given in Table 6, it can be seen that

(i) The triplet quantum yields of the phenols studied are smaller in cyclohexane than in acetonitrile and ethanol, whereas ethanol exhibits the highest triplet yields.

(ii) The unsubstituted phenol and the mono-*tert*-butyl forms substituted in the meta- or para-position show comparable quantum yields.

(iii) Practically no solvent effect is observed for 3,5-DTBP, 4-MeOP, and 2,4,6-TMeP.

(iv) In the case of 4-CNP, the triplet was only characterized by the sensitization experiment. A direct observation by excitation with 266 nm photons failed, in contrast to the other phenols.

(v) Most importantly, no ISC was found to proceed for 2,6-DTBP or 2,4,6-TTBP (the sterically hindered phenols), i.e., neither direct observation of triplets in the UV range nor the sensitization experiment (10) were successful.

(vi) From the literature,<sup>8</sup> the triplet quantum yields are similar for methylated phenols solved in *n*-hexane and in 3-methylpentane.

Normally, the nonradiative transition between the two spin systems (ISC) is relatively fast depending of the  $S_1-T_1$  energy difference (energy gap law<sup>17</sup>) of the states. However, compared to the internal conversion (IC), intersystem crossing (ISC) could be slower by as much as a few orders of magnitude.<sup>17</sup>

**Quantum Yields of the Photodissociation of the O–H Bond of ArOH( $S_1$ ).** In the photophysics of phenols, phenoxyl radicals have always been observed,<sup>1,3,4,8,22,23</sup> which are assumed to originate from the first excited singlet state under low excitation energy conditions (reaction 4) and via the deprotonation of the intermediate phenol radical cation under two photon excitation conditions at  $>0.5$  mJ laser power (cf. reaction 6). Using 266 nm photons and low energy ( $\sim 0.5$  mJ per pulse), we obtained only the photoexcitation of the phenol. To quantify dissociation quantum yields, we looked for direct access to the phenoxyl radical properties ( $\epsilon_T$ ), which mainly comprise by its typical optical absorption band around 400 nm. Therefore, for the maximum absorption of this band the extinction coefficients were determined in an independent way<sup>24</sup> provided by the monophotonic photoionization of phenolate (reaction 6b), known to take place quantitatively.<sup>25</sup> In these experiments, because of its well-known  $\epsilon_T$  value, the solvated electron could be used as an internal standard. Relating the electron and the phenoxyl radical absorption, the extinction coefficients of ArO $\cdot$  were determined in alkaline aqueous solution (see Table 7). To adjust



the absorption coefficient for the other solvents used, the half-width (fwhm) of the absorption bands at 400 nm was compared with that measured in aqueous solution. Because of the low solubility of some phenols, in the case of 2,4-DTBP (10 vol % *tert*-BuOH) and 3,5-DTBP (2 vol % EtOH), small amounts of alcohol were added. The sterically hindered phenols (2,6-DTBP, 2,4,6-TTBP) are not sufficiently soluble in water.

With the extinction coefficients determined, the quantum yields of photodissociation  $\Phi_D$  (reactions 4) were estimated for cyclohexane solutions. In a crude approximation and because of the low values, we assumed the same data for ethanol and acetonitrile as determined for cyclohexane. From the data given in Table 8, it can be seen that the dissociation quantum yields are markedly dependent on the phenol substitution pattern but are always still below 10%.

Finally, the question remains of whether phenol triplet states contribute to the formation of phenoxy radicals, in analogy to ketone triplets (cf. ref 26). To answer this, 1,3-cyclohexadiene, a typical triplet quencher, was added to solutions of phenol or 3-TBP in cyclohexane. Assuming that the absorption at 400 nm belongs mainly to the phenoxy radical and only partly to the phenol triplet state and that at 430 nm mainly the triplet absorbs, the contribution of phenoxy radicals formed via an imaginable dissociation of a phenol triplet could be judged. However, the quenching experiments described gave no evidence of phenoxy radical formation via the first excited triplet state in cyclohexane.

**Deactivation of Phenol First Excited Singlet States by Internal Conversion (IC).** The remaining process is the radiationless deactivation from the first excited singlet ( $S_1$ ) to the singlet ground state ( $S_0$ ) occurring via *internal conversion* (IC). Here the excitation energy is consumed by changes in the molecular geometry or is dissipated to the surroundings. The overall IC process can be understood in terms of the rate-controlling resonance interaction (RI) between the  $S_1$ - and the  $S_0$ -vibration levels followed by rapid vibration relaxation (VR). In contrast to the other relaxation channels studied there is no direct measure of the internal conversion efficiency (reaction 2). Using the exact and quantitative data of all the other competing  $\text{ArOH}(S_1)$  deactivation processes, the quantum yield difference from the total gives the fraction or the internal conversion  $\Phi_{IC} = \Phi_{RI} + \Phi_{VR} = [1 - \Phi_T + \Phi_f + \Phi_D]$ . These data are given in Table 8 together with the experimentally determined quantum yields of the deactivation channels studied described in the previous chapter estimated for cyclohexane, acetonitrile and ethanol solutions. Although the approach used cannot distinguish between the RI and VR contribution, for physical reasons the vibration relaxation is nearly unaffected by the influences considered, whereas relaxation by resonance interaction depends on the overlap of the corresponding vibration levels (Franck–Condon factors).

It can be seen that the phenol singlet state relaxation behavior depends on both the solvent nature and the substitution pattern of the phenols. If at all possible with our data set, it can be stated that  $\Phi_{IC}$  is considerably higher in the nonpolar cyclohexane than in acetonitrile and ethanol as polar solvents. This effect is very pronounced for phenol itself where the IC yield amounts to 0.58 in cyclohexane, 0.27 in acetonitrile, and only 0.07 in ethanol (cf. Table 8). Certainly, ethanol as protic medium already plays a special role with respect to hydrogen bonding with the phenol group in the singlet ground state.

Analyzing the effects of substitution at the aromatic moiety, in the cases of phenol and its meta- and para-alkyl-substituted derivatives and also for 2,4,6-TMeP, all these varied substances show comparable photophysical characteristics. This means that

the trend interpretation could be made similar for all of them and that the quantum yield of internal conversion  $\Phi_{IC}$  ranges from 0.15 to 0.70. Using the data of Table 8 and also of Tables 1 and 2 (taking singlet lifetime  $\tau_f$  as a crude measure for characterizing radiationless deactivation), the following trends could be derived from an in more detailed analysis:

(i) As the degree of alkyl substitution increases, so does the quantum yield of IC. This holds in particular for the bulky substituents, i.e., for *tert*-butyl groups.

(ii) In cyclohexane, as near as the bulky substituents are to the phenoxy group,  $\Phi_{IC}$  also increases at the expense of the radiative processes.

(iii) As an extreme case, 2,6-di-*tert*-butyl substitution leads to a quantitative internal conversion, already indicated by the very short fluorescence lifetimes between 50 and 250 ps.

(iv) From single up to triple methyl substitution, the effects observed are not as pronounced as those discussed for *tert*-butyl groups. This also seems to hold for methoxy substituents.

(v) With increasing solvent polarity, the yield of the radiationless internal conversion decreases and the radiative channel (in particular fluorescence) becomes more dominant, except for the sterically hindered phenols.

The two sterically hindered phenols with *tert*-butyl substituents in both ortho positions behave quite differently from the other phenols discussed above. Here the triplet quantum yield was found to be zero, and also the yields of fluorescence and dissociation are negligible for all solvents used. Consequently, the quantum yield for the internal conversion [ $1 - \Phi_T + \Phi_f + \Phi_D$ ] appears to be nearly unity. Assuming a similar ISC behavior (reaction 3) for all investigated phenols, the efficient IC (2) also arises because of their extremely short fluorescence lifetimes in the picosecond range, which are dramatically shorter than those of the other phenols. This has to be analyzed in detail for 2,6-DTBP and 2,4,6-TTBP (see Table 8) and is indicated by short-lived fluorescence for two other examples (4-Me-2,6-DTBP, IRGANOX-1076, cf. Table 2). This special behavior of the sterically hindered phenols enables them to be extremely good light quenchers.<sup>27</sup>

To obtain a deeper insight, we studied the IR spectra of phenol and 2,4,6-TMeP. In accordance with our hypothesis, the listed sterically hindered phenol 4-Me-2,6-DTBP shows a pronounced band at around 3600  $\text{cm}^{-1}$ , which can be attributed to the O–H-vibration modes.<sup>15</sup> By contrast, for phenol this band is much smaller by a factor of about ten.<sup>15</sup> Strong OH-vibrations increase the probability of nonradiative singlet state deactivation by internal conversion via efficient resonance interaction between the singlet excited state levels and the ground state OH-overtone.

For orientation, the IC behavior of two hetero group substituted phenols (4-cyano-, 4-methoxy-) was also studied. The compound 4-CNP exhibits very intense fluorescence and efficient triplet formation which together far dominate the relaxation of the first excited singlet state. It was found that the relation between fluorescence (reaction 1) and triplet formation (reaction 3) depends strongly on the polarity of the solvent. Surprisingly, internal conversion (reaction 2) was found to only play a negligible role (see Table 8). Somewhat differently, the electron-donating substitution in 4-MeOP always causes high ISC (0.55 to 0.67), low fluorescence probability (about 0.11) and internal conversion with  $\Phi_{IC} = 0.16$  to 0.30. As for the other phenols, dissociation (reaction 4) is merely of minor importance (around 0.05).

For all the phenols investigated, plotting the yields for the IC vs the corresponding measured fluorescence lifetimes within

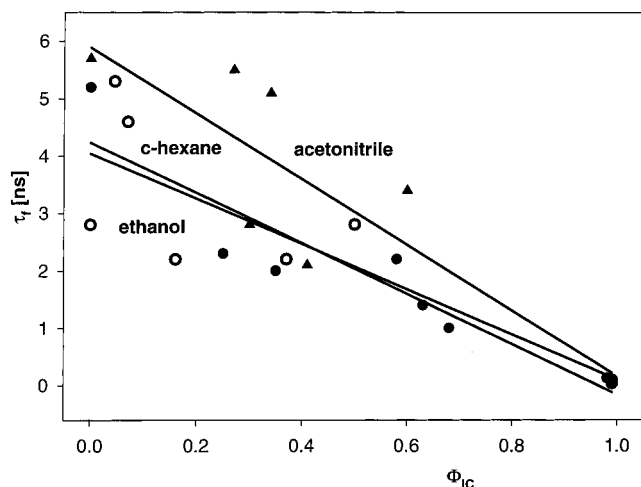


**Figure 5.** Relation between measured fluorescence lifetime and quantum yield of the internal conversion for the phenols studied in ethanol, cyclohexane, and acetonitrile.

all uncertainties yields a straight-line type correlation for cyclohexane, acetonitrile, and ethanol as solvents (cf. Figure 5).

**Interpreting Quantitatively Internal Conversion of Sterically Hindered Phenols with Quantum-Chemical-Based Considerations.** To understand the unusually short experimental singlet lifetimes of the sterically hindered and highly substituted phenols (e.g., 2,6-DTBP and 2,4,6-TTBP), we applied the theory of radiationless transitions.<sup>28</sup> At first sight, compared to the other phenols, the extreme shortening of the lifetime of the first excited singlet state (by a factor exceeding 10) cannot be understood solely as efficient internal conversion (IC) from  $S_1$  to  $S_0$  proceeding by an energy transfer to the resonance overtones of high-frequency oscillators (CH- and OH-groups). Normally, such an IC should be negligibly small, mainly because of the large energy gap between  $S_0$  and  $S_1$  ( $35000\text{ cm}^{-1}$  for phenol) and also because of the very weak intensity of the vibrational overtones in this region. Hence, intersystem crossing (ISC) ought to compete efficiently with fluorescence and could often dominate as the main channel of internal physical quenching of first excited singlet states.

The probability of ISC is especially large for molecules with a second triplet level below the first excited singlet level. Then the radiationless transition  $S_1-T_1$  can take place either by direct spin-orbital coupling of  $S_1$  to the higher vibrational level of  $T_1$  or by spin-orbital coupling to one of the higher  $T_n$  states followed by rapid internal conversion  $T_n-T_1$ , where the efficiency of ISC depends on the extent of the spin-orbital coupling as well as the energy gap between the states involved.<sup>17</sup> This seems to be valid in our case ( $T_1$  energy of phenol is  $28500\text{ cm}^{-1}$ ,  $\Delta E(S_1-T_1) = 6500\text{ cm}^{-1}$ ). Furthermore, as calculated for phenols with the time-dependent density functional theory (TDFT) method,<sup>29</sup> the second and third triplet states of phenol lie below but near the  $S_1$  state. As a result, most of the  $S_1$  excitation energy ought to be deactivated through the ISC channel.

However, the quantum chemical calculation showed that the  $S_1$  and  $T_1-T_3$  electronic states of phenol are mostly formed by the excitation of electrons from the two highest occupied  $\pi$ -MO's to the two lowest  $\pi$ -MO's. Yet according to the selection criteria for ISC known as Sayed's rules,<sup>17</sup> transitions  $^1(\pi, \pi^*) \leftrightarrow ^3(\pi, \pi^*)$  are forbidden.

Furthermore, it has been calculated that the valence HOMO  $\pi$ -electrons of phenols taking part in the formation of  $S_1$  and  $T_1$  excited states are distributed throughout the aromatic ring

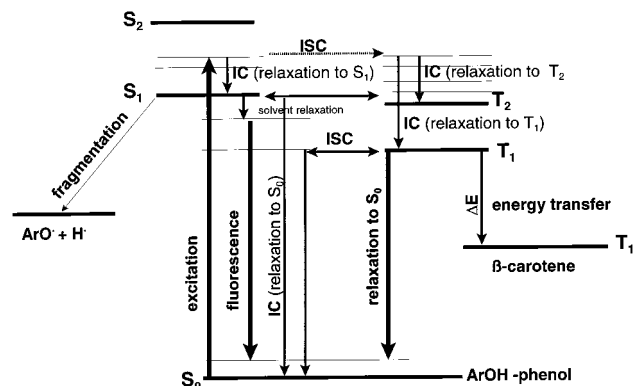


**Figure 6.** Jablonski scheme adapted for the phenol excited-state relaxation.

with a maximum electron density at position  $C_1$  and up to 20% electron density on the phenolic oxygen atom. Because the valence OH oscillator is very close to the  $\pi$ -electron density, it is obvious that the intensity of the valence O-H-vibration plays an important role in the radiationless deactivation. Comparison of the geometrical parameters calculated and the vibration spectra of all the phenols studied resulted for the sterically hindered phenols (2,6-DTBP and 2,4,6-TTBP) in the methyl H-atoms of the bulky groups being close to the OH-group (about  $2.2\text{ \AA}$  distance), enabling interaction with an oxygen lone electron pair or the formation of something like a hydrogen bond. Consequently, vibrations of the phenolic group ought to be strongly influenced and therefore the IC route efficiency increases.

For interpreting the IR spectra, a quantum chemical-based frequency analysis has been performed showing an up to 8-fold increase in the intensity of the high energy valence O-H-vibration (at around  $3600\text{ cm}^{-1}$ ) for the sterically hindered phenols. This increase in intensity is connected to a decrease in the OH torsion vibration, which indicates a strong interatomic interaction too. The enhanced intensity of the valence OH-vibration strengthens overlapping between vibration levels, i.e., an increase in the Franck-Condon factor. Therefore, radiationless transitions between  $S_1$  and  $S_0$  states are more likely. In contrast to the other phenols, in the sterically hindered molecules the very intensive high-energy valence O-H-vibration stimulates the intensity of the overtones, and efficient overlapping with fluorescence spectra improves resonance between the levels (Franck-Condon principle), resulting in very efficient internal conversion as in the case of the sterically hindered phenols. This situation can be understood by considering the intensity values calculated, given in Table 3.

## Concluding Discussion

As initially formulated by a more chemically based competition mechanism (reactions 1–5), the relaxation of the first excited singlet state of the phenols can also be visualized by an adopted common Jablonski scheme (shown in Figure 6), which better reflects the energetics of the relaxation reactions. Excitation brings the molecule from the ground-state  $S_0$  to a vibrationally excited level of  $S_1$ . As known for all of the vibration relaxations considered, the relaxation to the first electronically excited level  $S_1$  (Kasha's rule, ref 30) takes place extremely fast ( $10^{13}\text{ s}^{-1}$ ). The  $\text{ArOH}(S_1)$  level is the central point where the processes 1–4 branch out. Because of the systematics of our study (cf. Table 8), it can be stated that reactions 1, 3, and 4 follow in a first approximation the same dynamic rules in identical surroundings and show similar kinetic parameters when

expressed as rates, e.g., in cyclohexane:  $k_{\text{rad}} = 4.5 \times 10^7 \text{ s}^{-1}$  (radiative decay),  $k_{\text{ISC}} = 10^8 \text{ s}^{-1}$ ,  $k_{\text{IC}} = 10^8 - 2 \times 10^{10} \text{ s}^{-1}$ , and  $k_{\text{D}} = 3 \times 10^7 \text{ s}^{-1}$ .

The main variation factor appears in the internal conversion caused by resonance interaction (reaction 2) of the  $S_1$  level with the  $S_0$ -vibration overtones. As discussed for the bulky substituted phenols (2,6-di-*tert*-butyl-) as an extreme case, by improving the Franck–Condon factor of this transition, the internal conversion rate (reaction 2) is drastically accelerated. Such an effect could also be responsible for the accelerated decay of the first excited singlet state of the 2-mono-*tert*-butyl-substituted compounds (2-TBP and 2,4-DTBP), at least in nonpolar solutions.

Certainly, other factors can also contribute to the IC efficiency. However, finding reasons for the gradually differing effects of the other substituents and in other positions of the phenol is a very speculative and complex task which we shall sidestep here.

Accepting the statement of the compatibility of processes 1, 3, and 4, from the systematics derived of the mainly directly characterized reaction channels (Table 8), we can use as a rough means for judging internal conversion (IC) the fluorescence lifetimes, which are measured for diverse phenols in this paper (Tables 1 and 2) and are partially available in the literature.

Another important effect is caused by the polarity of the solvents. Depending on polarity and also in protic solvents, the lifetime of the phenol first excited singlet state lengthens (e.g. up to 5 ns). Moreover, there is a relatively steep step from cyclohexane to *n*-butyl chloride. Yet there are also examples where singlet lifetimes are quite constant for all the solvents (2,4,6-TMeP, 4-MeOP). Hence our formal systematization seems to contain exceptions. The singlet lifetime in aqueous solution is clearly different for nearly all cases, which was found to be generally lower than for alcohols as solvent.

Finally we again refer to the special photophysical properties of the sterically hindered phenols. In these compounds the relaxation of the first excited singlet state proceeds exclusively by internal conversion, irrespective of the solvent properties. According to quantum chemical-based considerations, the exceptional role of the sterically hindered phenols seems to be caused by the very efficient coupling between  $\text{ArOH}(S_1)$  and the overtones of  $\text{ArOH}(S_0)$ . This makes the sterically hindered phenols ideal, complete light quenchers, and partly explains their excellent antioxidant action.<sup>27</sup>

## References and Notes

- Land, E. J.; Porter, P.; Strachan, E. *Trans. Far. Soc.* **1961**, *57*, 1885; Land, E. J.; Porter, G. *Trans. Faraday Soc.* **1963**, *59*, 2016.
- Shukla, D.; Schepp, N. P.; Mathivanan, N.; Johnston, L. J. *Can. J. Chem.* **1997**, *75*, 1820.
- Dellonte, S.; Marconi, G.; Monti, S. *J. Photochem.* **1987**, *39*, 33.
- Bent, D. V.; Hayon, E. *J. Am. Chem. Soc.* **1975**, *97*, 2599.
- Grabner, G.; Köhler, G.; Zechner, J.; Getoff, N. *J. Phys. Chem.* **1980**, *34*, 3000.
- Dellonte, S.; Marconi, G. *J. Photochem.* **1985**, *30*, 37.
- Köhler, G.; Rechthaler, K. *Pure Appl. Chem.* **1993**, *65*, 1647.
- Grabner, G.; Köhler, G.; Marconi, G.; Monti, S.; Venuti, E. *J. Phys. Chem.* **1990**, *94*, 3609.
- Häupl, T.; Windolph, C.; Jochum, T.; Brede, O.; Hermann, R. *Chem. Phys. Lett.* **1997**, *280*, 520.
- Frisch, M. J.; Trucks, G. W.; Schlegel, H. B.; Scuseria, G. E.; Robb, M. A.; Cheeseman, J. R.; Zakrzewski, V. G.; Montgomery, A.; Stratmann, R. E.; Burant, J. C.; Dapprich, S.; Millam, J. M.; Daniels, A. D.; Kudin, K. N.; Strain, M. C.; Farkas, O.; Tomasi, J.; Barone, V.; Cossi, M.; Cammi, R.; Mennucci, B.; Pomelli, C.; Adamo, C.; Clifford, S.; Ochterski, J.; Petersson, G. A.; Ayala, P. Y.; Cui, Q.; Morokuma, K.; Malick, D. K.; Rabuck, A. D.; Raghavachari, K.; Foresman, J. B.; Cioslowski, J.; Ortiz, J. V.; Baboul, A. G.; Stefanov, B. B.; Liu, G.; Liashenko, A.; Piskorz, P.; Komaromi, I.; Gomperts, R.; Martin, R. L.; Fox, D. J.; Keith, T.; Al-Laham, M. A.; Peng, C. Y.; Nanayakkara, A.; Gonzalez, C.; Challacombe, M.; Gill, P. M. W.; Johnson, B.; Chen, W.; Wong, M. W.; Andres, J. L.; Head Gordon, M.; Replogle, E. S.; Pople, J. A. *Gaussian 98*, Revision A.9; Gaussian, Inc.: Pittsburgh, PA, 1998.
- Becke, A. D. *J. Chem. Phys.* **1993**, *98*, 5648; Becke, A. D. *J. Chem. Phys.* **1996**, *104*, 1040.
- Reichardt, C. *Solvents and Solvent Effects in Organic Chemistry*; VCH Verlagsgesellschaft mbH: Weinheim, 1990.
- Mataga, N.; Kaifu, Y.; Koizumi, M., *Bull. Chem. Soc. Jpn.* **1956**, *29*, 465 and references therein.
- Lakowicz, J. R. *Principles of Fluorescence Spectroscopy*; Plenum Press: New York, 1983.
- Schrader, B. *Raman/Infrared Atlas of Organic Compounds*; VCH Verlagsgesellschaft: Weinheim, Germany, 1989.
- Strickler, S. J.; Berg, R. A., *J. Chem. Phys.* **1962**, *37*, 814.
- Klessinger, M.; Michl, J. *Lichtabsorption und Photochemie organischer Molekül*; VCH Verlagsgesellschaft: Weinheim, Germany, 1989.
- Murov, S. L.; Carmichael, I.; Hug, G. L., *Handbook of Photochemistry*, 2nd ed.; Marcel Dekker: New York, 1993.
- Bensasson, R.; Land, E. J. *Trans. Faraday Soc.* **1971**, *67*, 1904. Amand, B.; Bensasson, R., *Chem. Phys. Lett.* **1975**, *34*, 44.
- Turro, N. J. *Modern Molecular Photochemistry*; University Science Books: Mill Valley, 1991.
- Köhler, G.; Kittel, G.; Getoff, N., *J. Photochem.* **1982**, *18*, 19.
- Brede, O.; Hermann, R.; Orthner, H. *J. Inf. Rec.* **1996**, *22*, 393. Brede, O.; Orthner, H.; Zubarev, V.; Hermann, R., *J. Phys. Chem.* **1996**, *100*, 7097.
- Hermann, R.; Naumov, S.; Mahalaxmi, G. R.; Brede, O. *Chem. Phys. Chem.* **2000**, *324*, 265. Hermann, R.; Naumov, S.; Brede, O. *J. Mol. Struct. (THEOCHEM)* **2000**, *532*, 69.
- Jochum, T. Thesis, University Leipzig, **1999**.
- Feitelson, J.; Hayon, E.; Treinin, A. *J. Am. Chem. Soc.* **1973**, *95*, 1025.
- Topp, M. R. *Chem. Phys. Lett.* **1975**, *32*, 144.
- Brede, O.; Naumov, S.; Hermann, R. *Chem. Phys. Lett.* **2002**. In press.
- Ermolaev, V. L.; Sveshnikova, E. B. *Russ. Chem. Rev.* **1994**, *63*, 905; Medvedev, E. S.; Osherov, V. I., *Radiationless Transitions in Polyatomic Molecules*; Springer-Verlag: Heidelberg, 1995.
- Bauerschmitt, R.; Ahlrichs, R. *Chem. Phys. Lett.* **1996**, *256*, 454.
- Kasha, M. *Discuss. Faraday Soc.* **1950**, *9*, 14